JGR Biogeosciences

RESEARCH ARTICLE
10.1029/2018JG004743

Special Section:
Biogeochemistry of Natural Organic Matter

The Molecular Composition of Humic Substances Isolated From Yedoma Permafrost and Alas Cores in the Eastern Siberian Arctic as Measured by Ultrahigh Resolution Mass Spectrometry

A. Zherebker[1,2,3], D. C. Podgorski[4], V. A. Kholodov[5], A. A. Orlov[1,3], N. V. Yaroslavtseva[5], O. Kharybin[1], A. Kholodov[6,7], V. Spector[8], R. G. M. Spencer[9], E. Nikolaev[1,2], and I. V. Perminova[3]

[1]Skolkovo Institute of Science and Technology, Skolkovo, Moscow, Russia, [2]Institute of Energy Problems of Chemical Physics, Russian Academy of Sciences, Moscow, Russia, [3]Department of Chemistry, Lomonosov Moscow State University, Moscow, Russia, [4]Department of Chemistry and Pontchartrain Institute for Environmental Sciences, University of New Orleans, New Orleans, LA, USA, [5]V.V. Dokuchaev Soil Science Institute, Moscow, Russia, [6]Geophysical Institute, University of Alaska, Fairbanks, AK, USA, [7]Institute of Physical-Chemical and Biological Problems in Soil Science, Russian Academy of Sciences, Moscow, Russia, [8]Melnikov Permafrost Institute of the Siberian Branch, Russian Academy of Sciences, Yakutsk, Russia, [9]National High Magnetic Field Laboratory Geochemistry Group and Department of Earth, Ocean, and Atmospheric Science, Florida State University, Tallahassee, FL, USA

Abstract Ongoing climate change is making the large pool of organic matter (OM) stored in Arctic permafrost vulnerable to mobilization; thus, garnering a deeper understanding of molecular transformations within the abundant pool of soil OM, specifically humic substances, is crucial. Here we present the first high-resolution mass-spectrometry examination of molecular compositions of humic acid (HA) and fulvic acid (FA) isolated from organic-rich deep yedoma (Pleistocene age ice-rich permafrost) and alas (thermokarst deposit formed during permafrost thaw) cores. The FA fractions were dominated by oxygen-rich unsaturated compounds, whereas the HA fractions were mostly composed of relatively reduced saturated and aromatic moieties. A substantial increase in contribution of both CHO-only and N-containing aliphatic compounds was observed in the HA fractions of the yedoma OM with depth, whereas the alas HA fractions were depleted in aliphatics but enriched with condensed and hydrolyzable tannins. The observed differences in compositional space of the immobile OM stored in the deep yedoma versus alas deposits were consistent with evolution of OM during thermokarst lake genesis, implying intense microbial degradation of N-rich OM released from the yedoma deposits and accumulation of highly degraded, plant-derived OM. The patterns of molecular transformations of OM were apparent in compositional space of the least degraded HA fractions as compared to much more oxidized FA fractions. This shows great promise of molecular exploration of the alkali-extracted OM, comprising up to 50% of the total organic carbon in deep permafrost both for paleoreconstructions and predictions of climate feedback to released OM due to permafrost thaw.

Key Points:
- Application of high-resolution mass spectrometry revealed significant contribution of reduced saturated compounds in permafrost humic acids
- Comparison of yedoma to alas humic fractions indicated substantial alteration of organic matter during thermokarst depression
- Extraction of humic acids enables much better imprint of evolutionary transformation of immobile organic matter during thaw events

Supporting Information:
- Supporting Information S1
- Table S1

Correspondence to:
E. Nikolaev and I. V. Perminova,
ennikolaev@rambler.ru;
iperm@med.chem.msu.ru

Citation:
Zherebker, A., Podgorski, D. C., Kholodov, V., Orlov, A. A., Yaroslavtseva, N. V., Kharybin, O., et al. (2019). The molecular composition of humic substances isolated from yedoma permafrost and alas cores in the eastern Siberian Arctic as measured by ultrahigh resolution mass spectrometry. *Journal of Geophysical Research: Biogeosciences*, *124*, 2432–2445. https://doi.org/10.1029/2018JG004743

Received 11 AUG 2018
Accepted 13 JUN 2019
Accepted article online 9 JUL 2019
Published online 5 AUG 2019

1. Introduction

Permafrost soils hold a large pool of ancient biolabile organic carbon (OC), which can be mobilized due to climate change (Tesi et al. 2016; Vonk et al., 2013). Arctic permafrost stores about 1,672 Pg of OC (Tamocai et al., 2009), and at least 450 Pg of OC is held in the so-called yedoma deposits in the Russian East Siberia (Zimov, Davydov, et al., 2006; Zimov, Schuur, & Chapin, 2006). Yedoma represents an organic-rich Pleistocene age ice-rich permafrost, which has about 2% OC by mass and an ice content of 50–90% by volume (Strauss et al., 2017). This makes yedoma deposits particularly susceptible to rapid thaw during warmer climatic periods. The thaw of yedoma over Holocene history leads to its local subsidence giving rise to formation of thermokarst lakes (Shmelev et al., 2017). The studies on evolution of the thermokarst lakes (Anthony et al., 2014) have shown their changing role in CH_4 and CO_2 emission: starting from strong CH_4 emission during thaw of Pleistocene yedoma sediments, followed by strong CO_2 uptake due to high primary productivity leading to formation of organic-rich Holocene sediments, and finally by establishing neutral (peatland type) gaseous exchange of alas sediments formed as a result of complete drain and refreezing of Holocene sediments. Hence, the regions of connected yedoma deposits and alas sediments are of

particular interest for exploring evolution of carbon cycling within the thermokarst lakes at the molecular level as reflected in the molecular composition of organic matter (OM) preserved in the deep layers of Pleistocene versus Holocene sediments. These deep permafrost OC storages create different feedbacks to climate change (Schirrmeister et al., 2011).

Substantial progress in understanding molecular composition of OM stored in permafrost has been achieved using Fourier transform ion cyclotron resonance mass spectrometry (FT-ICR MS), which has the highest resolving power (>400,000 at m/z 400) and mass accuracy (<1 ppm) among all mass-spectrometry techniques (D'Andrilli et al., 2013; Marshall et al., 1998). Recent studies utilizing FT-ICR MS have revealed alterations in the surface layer of permafrost OM with seasonality (Choi et al., 2017). Distinct molecular signatures of permafrost-dominated OM in Arctic fluvial systems were examined by Perminova et al. (2014) and Spencer et al. (2015). These studies highlighted the relative contribution of molecular formulae with a high H/C ratio derived from permafrost OM, which are energy rich and thus biolabile (Rossel et al., 2013). High bioavailability of OM released from yedoma permafrost thaw was also reported by Mann et al. (2012), 2015) and Vonk et al. (2015). In addition, the dominance of microbial over photochemical processing of dissolved organic matter (DOM) in the Kolyma River Basin was revealed by Stubbins et al. (2017). The latter findings are indicative of a smaller contribution of photochemically active aromatic units into the molecular ensemble of yedoma permafrost OM.

However, all the above noted studies on the molecular composition of OM stored in permafrost were conducted on the relatively small portion of water-soluble DOM (<10% of the total OC) released during permafrost thaw (Qualls & Haines, 1992). At the same time, the much larger portion of less oxidized and, hence, less water soluble OC is stored in the permafrost in the pool of immobile OM, which can be released from the sediments using alkali extraction (Vasilevich et al., 2018). This alkali-extracted OM is traditionally referred to as humic substances (HSs) and comprises more than 50 % of soil OM (Stevenson, 1995). We have not found to date a single report on the compositional space of HS extracted from permafrost in the region of interest. We hypothesized that utilization of alkali extraction will enable identification of the least transformed components within OM stored in deep yedoma and alas sediments, which cannot be found in DOM. This will therefore provide a much clearer view on the evolution of the molecular ensemble of the total OM during permafrost thaw. For this purpose, we extracted HS from the cores of diagenetically connected yedoma and alas sediments from the Shchuchye Lake region, Kolyma River Basin, Northeast Siberia. The further fractionation of HS into the acid-insoluble fraction of humic acids (HAs) and acid-soluble fraction of fulvic acids (FAs) was conducted to enable better ionization of the less oxidized HA fraction. The high-resolution mass spectrometer was also used for improved identification of molecular components of this fraction. The obtained results were to provide deeper insight into differences/similarities of molecular compositions of yedoma and alas OM enhancing our knowledge on the molecular evolution of OM during the past and future thaw periods.

2. Methods

2.1. Site Description

The HS were isolated from two deep (down to 16 m) permafrost cores obtained in July 2012 and 2013 from boreholes drilled using a UKB-12/25 rotary drill rig near Shchuchye Lake and the town of Chersky (Figure 1; Sakha Republic, Yakutia, Russia). The first core (#12-01) was taken from a hilltop (68.744825°N, 161.383834°E) and recovered the syncryogenic deposits of yedoma. These types of deposits were accumulated during the Late Pleistocene under severe cold climatic conditions (Strauss et al., 2017). Due to the specific mechanism of their formation when the deposits were freezing concurrent with sedimentation, and because of the low rate of OM decomposition, these deposits contain vast amounts of poorly degraded OM (Zhu et al., 2016). The core spans the section of deposits that can be divided into three horizons. The deepest (Unit 1) corresponding to the depth interval 9 to 15 m had been formed under the conditions of dry grassy shrub tundra steep. Sedimentation of Unit 2 (2–9 m) took place in a wet cold environment within a peat wetland. Unit 3 lays right under the seasonally thawed layer up to a depth of 2 m and represents the so called cover, or transient layer, which was thawed from the top during the Holocene climatic optimum and then refrozen due to climate cooling.

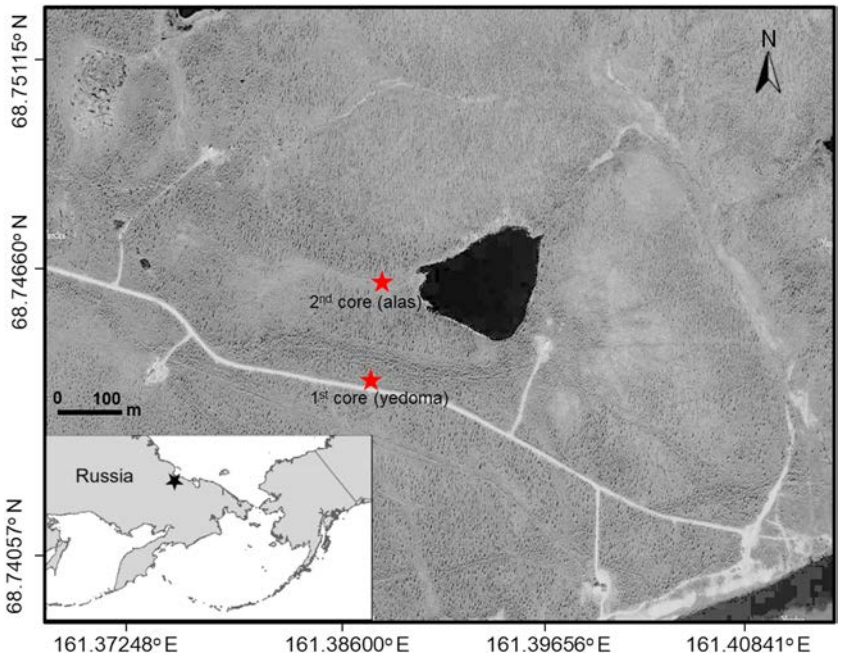

Figure 1. Map of the borehole selection in the vicinity of the North East Siberian Station of Russian Academy of Sciences.

The second core (#13-02) was collected within a thermokarst depression (also known as alas) approximately 250 m northeast from the first core (68.746207°N, 161.388074°E). This depression was formed due to the thawing of ice-rich yedoma deposits. The thawing was accompanied by surface subsidence from melting of massive ice bodies and compacting of associated deposits. This complex consists of a layer of lacustrine deposits in the upper part corresponding to the depth interval of the core from the surface to 2 m. This layer is underlined by the taberal deposits (original yedoma deposits, which have been thawed, compacted, and refrozen after the lake drainage or migration) covering the section of the core from 2 to 15 m. Organic material in these deposits was subjected to transformation and partial decomposition under anaerobic conditions during several thousands of years. Detailed core descriptions were reported in Webb et al. (2017). The samples for HS isolation were collected at different depths (Table 1), and we aimed to sample the major identified cryostratigraphic horizons. Samples Y3 and Y6 are characteristic of Unit 2 and Samples Y12 and Y15 Unit 1 of the yedoma core. Samples A13 and A15 represent the lower part of the layer of taberal deposits in the alas core. Comparing the composition of OM isolated from the original yedoma and the taberal deposits, we can examine how the process of thermokarst formation affects transformation of OM. All permafrost samples were kept frozen until OM extraction. The determination of OM content by combustion of dried soils (up to 4% of OM) and primary characterization of cores were performed previously (Webb et al., 2017). OC

Table 1
A List of the Core Samples of Permafrost Used for HA and FA Isolation and Their Characteristics With Regard to the Content of Organic Carbon and HS

Type of core	Depth of core, m	Site	%OC	HS yield, %	FA1, %	FA2, %	HA, %	C_{HA}/C_{FA}[a]
Yedoma	3.24–3.27	Y3	1.01	0.43	0.08	0.12	0.23	1.15
	6.26–6.3	Y6	1.38	0.39	0.07	0.1	0.21	1.21
	12.79–12.82	Y12	1.33	0.24	0.06	0.08	0.1	0.7
	15.08–15.10	Y15	0.66	0.21	0.06	0.07	0.08	0.65
Alas	13.03–13.10	A13	1.47	0.46	0.08	0.08	0.3	1.8
	15.12–15.18	A15	1.57	0.57	0.02	0.05	0.5	7

Note. HA = humic acid; FA = fulvic acid; HS = humic substance; OC = organic carbon.
[a]C_{HA}/C_{FA} ratio was calculated using the sum of FAs content: FA = FA1 + FA2. These ratios are given only for better data representation. The obtained values cannot be compared to the common C_{HA}/C_{FA} estimates while the isolation efficiency of FA with a use of PPL SPE cartridges does not exceed 60–70% (Dittmar et al., 2008). Hence, the data have a systematic bias towards magnification of the HA contribution.

content (%TOC) was determined using a total OC analyzer TOC-L series (Shimadzu) equipped with a SSM-5000A solid sample module.

2.2. Extraction of HSs

Fifty grams of each sampled layer of the permafrost cores were thawed in the dark at room temperature (20 °C) in a sterile polypropylene centrifuge tube and subsequently centrifuged (15 min, 10,000 rpm) in order to remove pore water and to avoid interference of DOM with HS. HA and FA extraction from the solid residue was undertaken following standard International Humic Substance Society protocols (Swift, 1996). All isolation steps were conducted under nitrogen. Each soil sample was first decalcified by adding 1 M HCl to create a soil slurry in water (1:10 by weight) until the pH value dropped down to 2. The acidified suspension was shaken for 6 hr and left for 16 hr. The supernatant was separated by centrifugation and used for the further extraction of the most hydrophilic fraction designated FA1. The residual decalcified soil was neutralized by adding 1 M NaOH to pH 7, and 0.1 M NaOH was then added to a final soil:water ratio of 1:10 (by weight). The suspension was shaken for 16 hr. Then, the alkaline supernatant was separated from the soil residues by centrifugation. The HA fraction was precipitated by acidification until pH 1-2 using 6 M HCl, and the HA precipitate was separated by centrifugation. The FA fraction was isolated from the supernatant as described below and designated FA2.

2.3. Purification and Isolation of HA and FA Fractions

The HA precipitate was redissolved in a minimum volume of 0.1 M KOH, and KCl was added to a K+ concentration of 0.3 M for coagulation of fine mineral particles (silt), which were removed by centrifugation. The HA fraction was precipitated again, and this time the precipitate was treated with a mixture of 0.1 M HCl and 0.3 M HF to remove finely dispersed silica-containing impurities in accordance with International Humic Substance Society protocols (Swift, 1996). The treated HA suspensions were purified by dialysis (4 kDa) until producing a negative Cl^- test with $AgNO_3$. The solid products were obtained by rotary evaporation to dryness.

The FA fractions (FA1 and FA2) were isolated according to the modified solid-phase extraction procedure as described elsewhere (Dittmar et al., 2008; Zherebker et al., 2016). In brief, a Bond Elut PPL cartridge (Megapack, 5 g) was activated by a consecutive discharge of 30 ml methanol and 30 ml 0.01M HCl prior to extraction. The acidified sample solution (pH 2) was passed through the activated cartridge at a flow rate of 6 ml/min. Then, the cartridge was washed with 50 ml of 0.01 M HCl for complete removal of salts and dried with a stream of nitrogen. The sorbed FAs were eluted with 50 ml of methanol at a flow rate of 2 ml/min. The collected dark brown eluate was rotor evaporated to dryness, and the solid products were stored in a freezer. In total, four and two sets of depth samples (HA, FA1, and FA2) were isolated from yedoma and alas cores, respectively. The final masses of all extracted samples are presented in Table 1.

2.4. Electrospray Ionization FT-ICR MS

Analysis of the FA fractions was performed using a FT-ICR MS Bruker Apex Ultra with harmonized cell (Bruker Daltonics) equipped with a 7 T superconducting magnet and electrospray ionization source housed at the Institute of Biomedical Chemistry of RAMS (Russia). The HA fractions were analyzed with a custom-built 9.4 T FT-ICR mass spectrometer equipped with a 22-cm diameter horizontal bore located at the National High Magnetic Field Laboratory (Tallahassee, Florida, USA). Implementation of the unique design simplifies access to the ion cyclotron resonance cell-improved detection sensitivity twofold (Kaiser et al., 2011), which is crucial for the analysis of HA due to low ionization efficiency of its components. Prior to analysis, the solid HA samples were treated three times by methanol/chloroform mixture (1:2) in order to remove lipids. Then they were dissolved in aqueous NH_3 (pH 10) followed by double dilution with methanol until a final concentration of 100 mg/L. The FA solutions were diluted with methanol to a concentration of 100 mg/L. All mass spectra were acquired in negative ionization mode by direct infusion at a flow rate of 90 μl/hr. A source heater temperature of 200 °C was maintained to ensure rapid desolvation in the ionized droplets. The electrospray ionization source needle voltage was −3,000 V. The spectra were obtained as 300 and 100 scan accumulation in cases of FA and HA, respectively. The number of scans for spectra acquisition was set according to the experimental sensitivity of the equipment. The resolution power was at least 530,000 at 400 m/z, which was achieved due to analytical capabilities of the harmonized cell (Nikolaev et al., 2011). The obtained mass spectra were externally calibrated on clusters of phosphoric acid in H_2O:MeOH (1:1), and

internal calibration was systematically conducted using the known peak series of OM reaching accuracy values <0.2 ppm.

Peaks with signal-to-noise ratio (S/N) >6 and their intensities were exported using DataAnalysis software (Bruker). The obtained mass lists were processed using the in-house "Transhumus" software designed by A. Grigoriev, which is based on a total mass difference statistics algorithm (Kunenkov et al., 2009). The generated CHONS formula was validated by setting chemical constraints (Koch et al., 2005): O/C ratio ≤1, H/C ratio ≤2.2, element counts (C ≤ 120, H ≤ 200, O ≤ 60, N ≤ 2, and S ≤ 1), and a mass accuracy window <0.5 ppm). Formulae were classified according to their stoichiometries (Hockaday et al., 2009): aliphatic (0 < O/C < 0.3 and 1.6 ≤ H/C < 2.2), N-saturated (1 ≤ N, 0.1 ≤ O/C < 0.65, and 1 ≤ H/C < 2.2), lignins (0.1 ≤O/C < 0.65 and 0.7 ≤ H/C < 1.6), condensed tannins (0 < O/C < 0.5 and 0.3 ≤ H/C < 0.7), hydrolysable tannins (0.5 ≤ O/C < 1, 0.3 ≤ H/C < 0.7, and 0.65 ≤ O/C < 1, 0.7 ≤ H/C < 1.3), and carbohydrates (0.65 ≤ O/C < 1 and 1.3 ≤ H/C < 2.2). Further quantification of the intensity-weighted population density of each class was performed as described by Perminova (2019) using the following expression:

$$D_k = \frac{\sum_{k=1}^{N_i} I_i}{\sum_{j=1}^{N} I_j}, k = 1, 2, ...n,$$

where D_k is the intensity-weighted population density of the class k; N is the total number of molecular formulae in each sample; N_k is the number of formulae belonging to the class k; I_j is the intensity of each peak with assigned formula; and I_i is the peak intensity of compound ion belonging to the class k. It should be stressed that throughout we avoid direct comparison of the intensities of molecular composition identified for HA and FA fractions because they were measured via different FT-ICR MS instruments.

2.5. Statistical Data Treatment

Statistical data processing was carried out using STATISTICA Base (StatSoft), Python 2.7, and R (https://www.r-project.org) scripts. For this purpose we created a list of molecular formulae identified in all samples. For the heatmap analysis, the molecular composition abundance fingerprints were generated for each sample. Principal component analysis (PCA) was performed including all 18 samples. A data matrix of unique molecular compositions was created for all samples using values 1 and 0 for presence and absence, respectively, as well as using intensity values. PCA was conducted according to Sleighter et al. (2010). For hierarchal cluster analysis (HCA), relative intensity averaged data for all samples were obtained:

$$(O/C)_w = \frac{\sum (O/C)_n * I_n}{\sum I_n}, (H/C)_w = \frac{\sum (H/C)_n * I_n}{\sum I_n}, DBE_w = \frac{\sum (DBE)_n * I_n}{\sum I_n}, C(H,N)_w = \frac{\sum C(H,N)_n * I_n}{\sum I_n},$$

where DBE = 1+0.5 (2C − H + N) and I the relative intensity of the corresponding peak in mass-spectrum. Samples were clustered according to Euclidean distances.

3. Results

3.1. Isolation of the Humic Fractions and Characteristics of Their Compositional Space

The %OC and masses of the HA and FA fractions are summarized in Figure 2 and Table 1. The total yield of the extracted HS from the yedoma cores ranged from 0.43% to 0.21% decreasing with depth (Table 1). In case of the alas core, the yields of HS were considerably higher and varied from 0.46% to 0.57% increasing with depth (Table 1). For the yedoma core, the highest mass yield of the HA fraction (115 mg) was observed for the upper layer (3 m). It decreased to 42 mg for 15-m sample as shown in Figure 2a. In the alas core, the higher yields for the HA fraction were observed for comparable depths: They accounted for 230 and 286 mg at depths of 13 and 15.5 m, respectively (Figure 2b and Table 1). The value of C_{HA}/C_{FA} ratio, which is indicative of the degree of humification of the OM, reduced drastically with depth in the case of the yedoma core: from 1.15 (~3 m) down to 0.65 (~15 m). Overall, the values of C_{HA}/C_{FA} ratio in the yedoma core at any depth were lower than those observed in the alas core: 1.8 and 7 for 13 and 15.5 m, respectively.

Up to ~3,700 and ~2,700 molecular formulae were identified in the FT-ICR mass spectra of FA and HA, respectively. The distributions of molecular compositions among the different heteroatom containing formulae are presented in Table 2. CHO formulae dominated molecular space of all HS fractions, which is

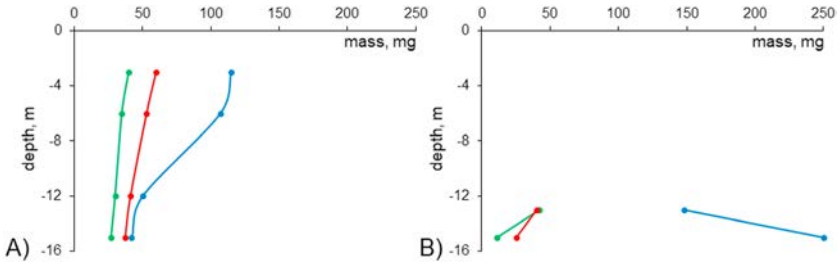

Figure 2. The mass yield of (a) yedoma and (b) alas humic substance fractions at different depths. Green, red, and blue colors correspond to FA1, FA2, and HA, respectively.

typical for soils (O'Donnell et al., 2016). In the yedoma core, the number of HA formulae decreased with depth from ~2,500 down to ~1,900. In both alas samples, ~2,500 molecular formulae were identified in the HA fractions, making them similar to the upper yedoma layer. All FA samples were characterized by the higher contribution of N-containing formulae (>30% of the total amount) as compared to HA samples (up to 20% of the total amount). A high content of N-containing compounds was reported previously for PPL-purified tundra soil DOM (Choi et al., 2017). The identified FT-ICR MS formula assignments were plotted in van Krevelen diagrams (Figure 3). A clear difference can be seen in the molecular assemblages of HA versus FA1 and FA2 fractions. All HA fractions have molecular constituents with the O/C values <0.5, whereas both types of FA fractions are dominated by the molecular constituents with O/C values >0.5. This is consistent with the solubility of FA in acids and indicative of the highly oxidized character of FA. On the contrary, HA fractions were characterized with the higher contributions of the saturated constituents (H/C >1.5) and condensed aromatics (H/C< 0.5). This provides for more aliphatic and hydrophobic character of the HA as compared to the FA.

Figure 4 shows the relative contribution of six predefined molecular classes (as shown in Figure 3): aliphatic species (I, $N = 0$), N-containing saturated species (II, $N > 0$), lignins (III), condensed tannins (IV), hydrolyzable tannins (V), and carbohydrates (VI), into compositional space of HA and FA (left and right panels, respectively) used in this study. The most substantial differences can be seen between the compositional space of the "deep layer" HA samples from yedoma versus the alas ones. While the yedoma HA was rich in aliphatic (up to 23%) and N-saturated compounds (2% and 4% for HA-Y-12.5 and HA-Y-15.5, respectively), the alas HA from the same depths were depleted with N-saturated compounds (<1%) but enriched with

Table 2
A List of the Isolated HS Samples, the Extracted Masses, and the Relative Contribution of $C_cH_hO_oN_nS_s$ Formulas Into Their Molecular Compositions

Core type	Sample	Mass (mg)	Number of assigned formulae	CHO (%)	CHON (%)	CHOS (%)	CHONS (%)
Yedoma 3 m	FA1-Y-3	40.5	2,791	1,661 (60)	893 (32)	162 (6)	75 (2)
	FA2-Y-3	60.0	1,935	1,178 (61)	710 (37)	45 (2)	2 (0)
	HA-Y-3	115.2	2,552	1,870 (73)	531 (21)	133 (5)	18 (1)
Yedoma 6.2 m	FA1-Y-6.2	35.2	3,400	1,950 (57)	941 (28)	456 (13)	53 (2)
	FA2-Y-6.2	53.1	3,281	1,789 (55)	1,024 (31)	429 (13)	39 (1)
	HA-Y-6.2	106.9	2,601	1,964 (75)	449 (17)	175 (7)	13 (1)
Yedoma 12.5 m	FA1-Y-12.5	29.7	2,017	1,204 (60)	509 (25)	265 (13)	39 (2)
	FA2-Y-12.5	41.4	2,305	1,383 (60)	782 (34)	133 (6)	7 (0)
	HA-Y-12.5	49.5	1,861	1,262 (68)	399 (21)	189 (10)	11 (1)
Yedoma 15 m	FA1-Y-15	27.0	2,356	1,520 (64)	706 (30)	108 (5)	22 (1)
	FA2-Y-15	36.9	2,999	1,544 (51)	1,066 (36)	344 (11)	45 (2)
	HA-Y-15	42.4	1,955	1,467 (75)	340 (17)	144 (7)	4 (1)
Alas 13 m	FA1-A-13	41.9	1,551	1,168 (75)	338 (22)	36 (2)	9 (1)
	FA2-A-13	40.0	2,653	1,547 (58)	813 (31)	238 (9)	55 (2)
	HA-A-13	148.4	2,726	1,958 (72)	529 (19)	226 (8)	13 (1)
Alas 15.5 m	FA1-A-15.5	11.0	2,872	1,783 (62)	840 (29)	230 (8)	19 (1)
	FA2-A-15.5	25.2	3,763	2,207 (59)	1,227 (33)	238 (6)	91 *n*(2)
	HA-A-15.5	250.2	2,511	1,958 (78)	504 (20)	49 (2)	0 (0)

Note. HA = humic acid; FA = fulvic acid; HS = humic substance.

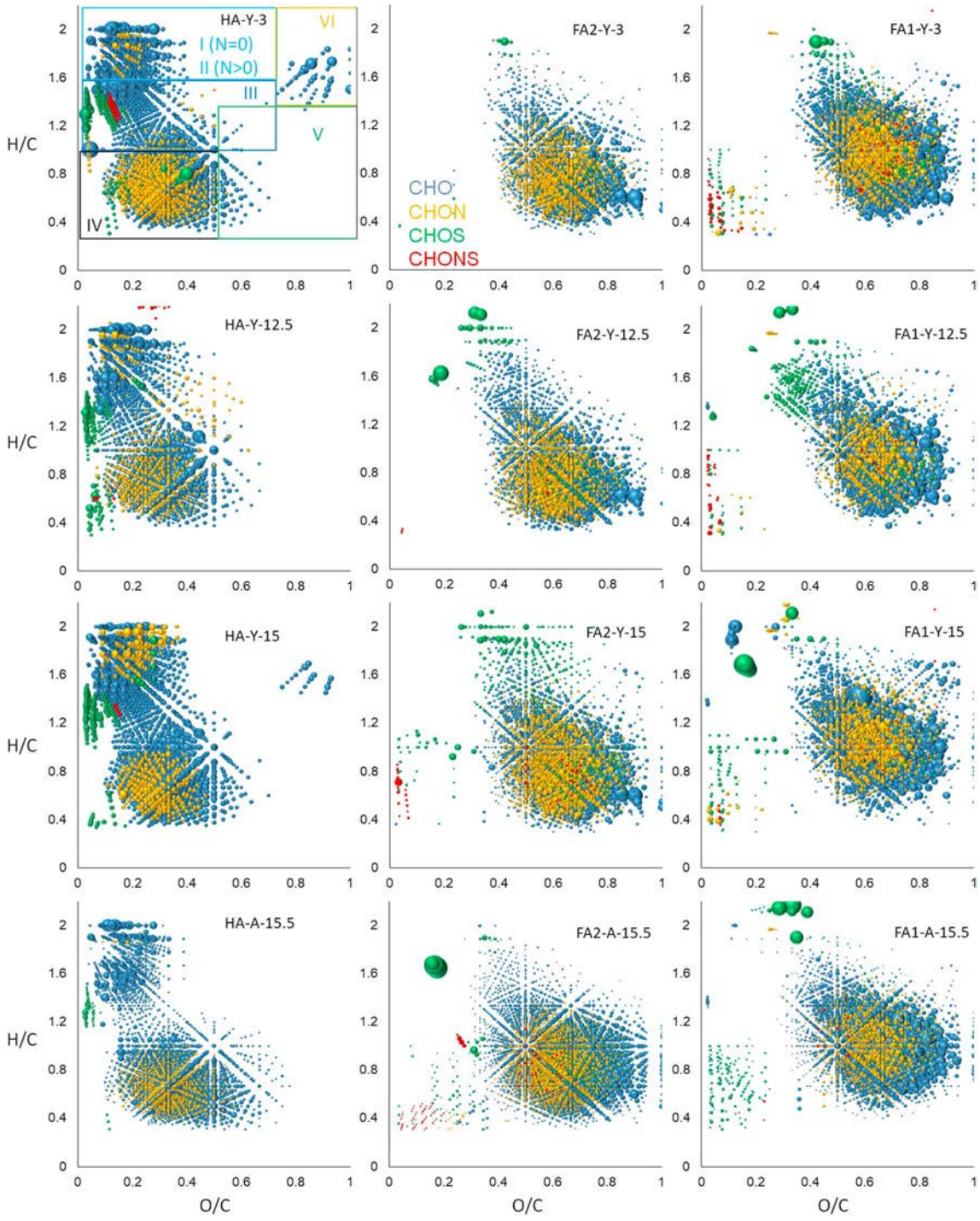

Figure 3. The van Krevelen diagrams plotted from the Fourier transform ion cyclotron resonance mass spectrometry formula assignments made for the HA, FA2, and FA1 fractions extracted from the Yedoma core collected at 3 m (HA/FA-Y-3), 12 m (HA/FA-Y-12.5), and 15 m (HA/FA-Y-15), and from the alas core at 15 m (HA/FA-A-15.5), from top to bottom, respectively. Roman numerals I–VI designate regions of aliphatic species, N-containing saturated species, lignins, condensed tannins, hydrolyzable tannins, and carbohydrates, respectively. HA = humic acid; FA = fulvic acid.

condensed and hydrolyzable tannins (43% and 6%, respectively). The FA fractions in both yedoma and alas cores were completely aromatic with the dominant contribution of lignins (up to 50% of the total formulae). The alas cores were characterized by a greater contribution of tannins versus the yedoma core, and of the hydrolysable tannins in particular.

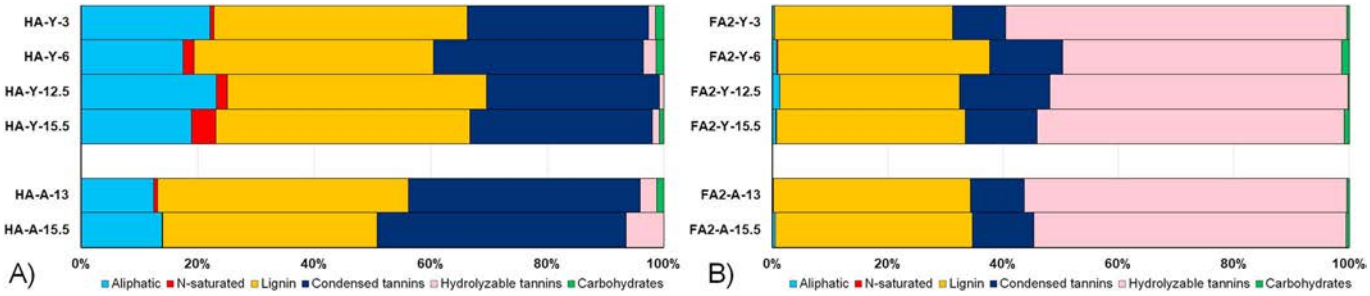

Figure 4. Relative contribution of different molecular classes (shown in the van Krevelen diagram; Figure 3a) for all fractions isolated from the yedoma and alas cores used in this study. HA = humic acid; FA = fulvic acid.

3.2. Statistical Analysis on FT-ICR MS Parameters of the Humic Fractions Under Study

All molecular formulae identified in the HA and FA samples used in this study and the calculated intensity-weighted average parameters (see data treatment) were used for constructing the heatmap plot and HCA dendrogram (Figure 5). Two distinct groups can be seen in the heatmap highlighted as a dark large square in the upper left corner produced by intercorrelations of all FA samples and as a dark smaller square in the bottom right corner produced by HA samples. This is indicative of a much stronger impact of the fractionation scheme (HA vs. FA) on molecular composition of the isolated HS as compared to the type and depth of the soil cores used in this study. The obtained data are in line with the dramatic differences between molecular space of HA and FA, which can be seen in Figure 3. Similarly, two major clusters (FA and HA) can be seen in the dendrogram (Figure 5b). In turn, the cluster of FA can be divided into two groups in line with the fractionation scheme resulting in three subgroups: FA1, FA2, and HA. This demonstrates again the crucial impact of the fractionation scheme on the molecular composition of the resultant OM.

The PCA provides information on the role of each variable in the sample groupings. The results of PCA based on Boolean fingerprints and formulae abundance are shown in Figure 6 and Table S2 in the supporting information. The first two components explain 58% of the variance in the data, with PC1 solely explaining 48% of the data variance (Figure 6a). The sample grouping is similar to the pattern observed in Figure 5b (HCA), confirming the strong impact of the fractionation procedure on compositional space of OM over the origin (alas or yedoma) and sampling depth. The contribution of specific molecular formulae into compositional space of the obtained grouping is shown in the corresponding van Krevelen diagrams (Figures 6b–6d). The plots show a distinct difference between the HA and FA fractions. The HA fractions (Figure 6b) were unique in high contributions of reduced molecules (with the higher values of H/C ratio) including lignins, aliphatic species (mostly, materials derived from linear terpenoids; Lam et al., 2007), and condensed tannins. The assigned formulae are typical of terrestrial and permafrost OM (Sleighter et al., 2010; Spencer et al., 2015). The FA1 fractions were unique in high contributions of relatively saturated oxidized molecules, which might be attributed to carboxyl rich alicyclic moieties (Hertkorn et al., 2007; Figure 6c). The high contribution of carboxyl rich alicyclic moieties is consistent with the isolation of the FA1 fractions by acidic extraction during the decalcification procedure. On the contrary, the alkali-extracted FA2 fractions were enriched with unsaturated oxidized components, for example, hydrolysable tannins (Figure 6d).

In order to explore the samples segregation with respect to the core depth, we undertook PCA within either HA or FA fractions using molecular formulae abundances. The resulting plots are shown in Figure 7. It can be seen that the use of relative peak intensities instead of Boolean fingerprints enabled us to distinguish FA2 and HA fractions extracted from the alas and deep yedoma cores. This PCA shows that all HS samples used in this study could be segregated into two groups: “deep alas and upper-layer yedoma” versus “deep yedoma,” which highlights the molecular connection between the degraded yedoma samples and the alas samples.

4. Discussion

4.1. General Features of Alkali-Extracted OM Isolated From the Yedoma and Alas Cores

The data on the yields of alkali-extracted OM (Table 1, Figure 2) obtained in this study have shown much higher content of this OM in the alas core as compared to the yedoma core. These data are consistent

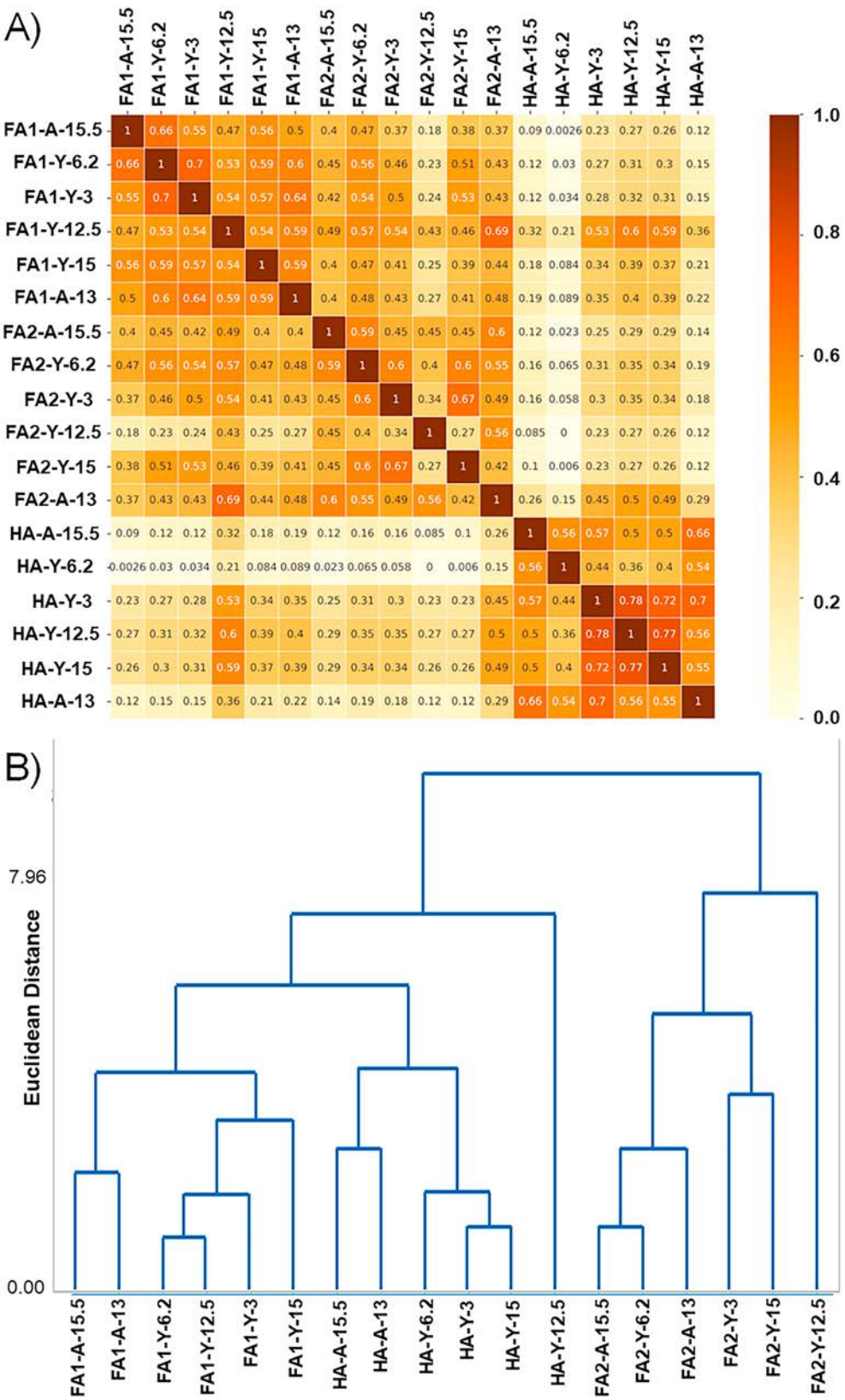

Figure 5. Statistical analysis of the Fourier transform ion cyclotron resonance mass spectrometry data obtained for the HA and FA fractions used in this study: (a) heatmap on the molecular formulae abundances; (b) hierarchal cluster analysis of intensity-weighted averaged parameters. HA = humic acid; FA = fulvic acid.

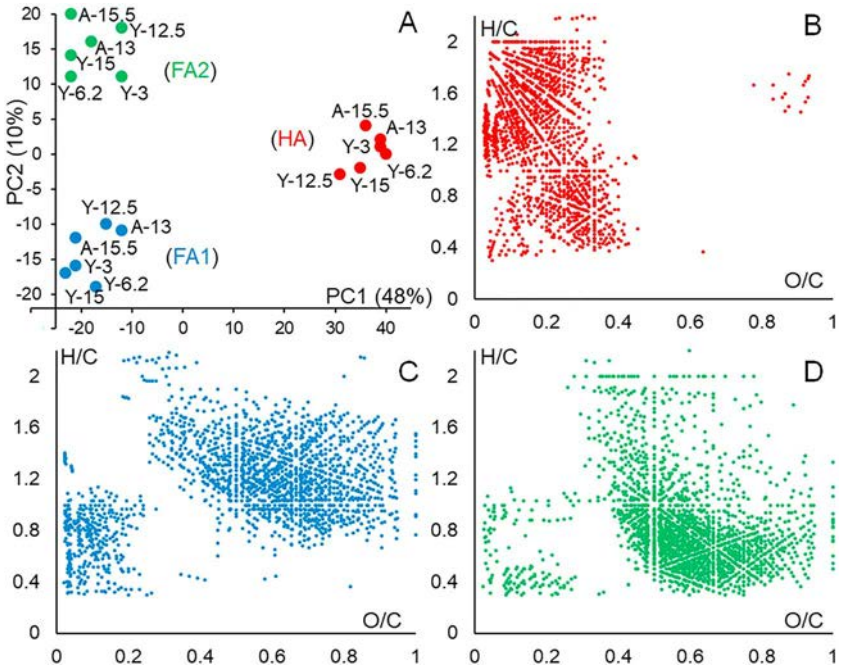

Figure 6. Principal component analysis plots of Fourier transform ion cyclotron resonance mass spectrometry data on Boolean fingerprints: (a) the plot of samples' scores, (b, c, and d) van Krevelen diagrams plotted for the molecular formulae contributed to HA (red), FA2 (green), and FA1 (blue). HA = humic acid; FA = fulvic acid.

with published results on the higher total carbon density in alas as compared to yedoma layers in the Kolyma River Basin (Shmelev et al., 2017; Webb et al., 2017). The higher rates of recent (Holocene) accumulation of OC within the alas sediment formed in the thermokarst lake might account for this difference (Anthony et al., 2014). It is also consistent with the reported findings on the substantially larger OC storage in alas and thermokarst soils as compared to undisturbed yedoma deposits (Shmelev et al., 2017; Siewert et al.,

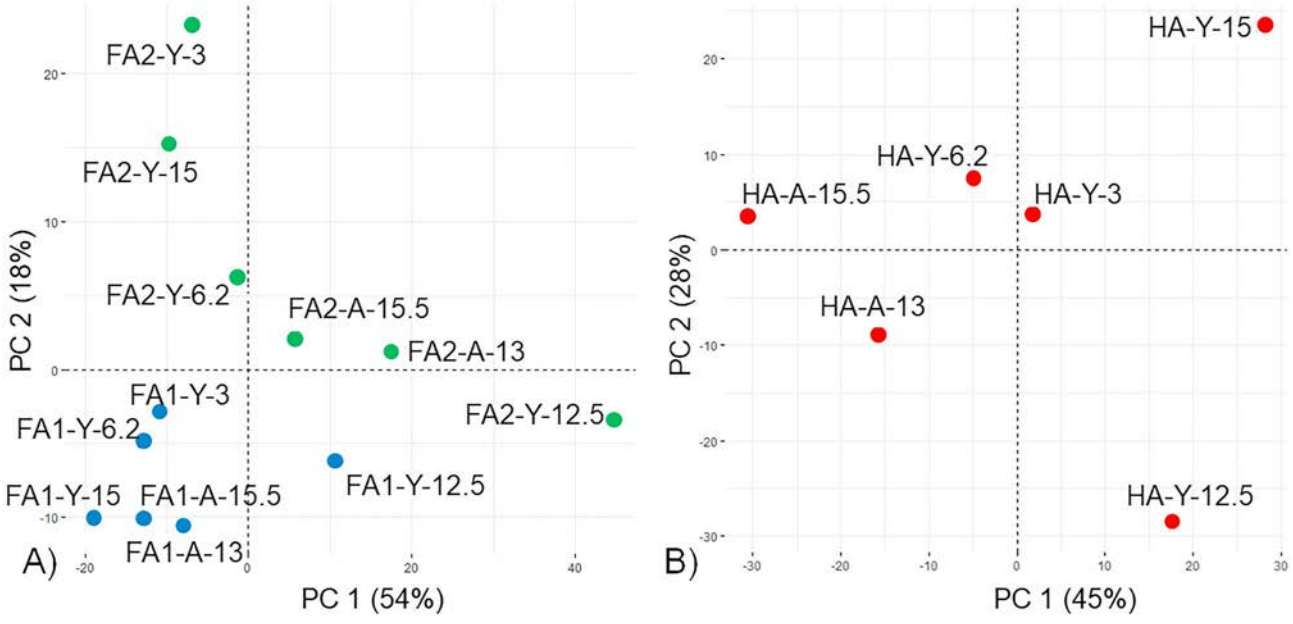

Figure 7. Principal component analysis plots of Fourier transform ion cyclotron resonance mass spectrometry data on molecular formulae abundance: (a) FA1 and FA2 fractions and (b) HA fractions. HA = humic acid; FA = fulvic acid.

2015; Strauss et al., 2013). The upper layers of the undisturbed yedoma core under study (Units 2 and 3) contained much more degraded OM with the higher humification index (C_{HA}/C_{FA} ratio) as compared to the deep permafrost layers from Unit 1 (13–15 m). This is consistent with reports of a higher transformation rate of OM in the upper layers of the yedoma deposits as compared to the deeper ones (Shirshova et al., 2009). Still, the highest value for the humification index (up to 7) was observed for OM in the deep layer of the alas core, which reflects the greater humification degree of the alas OM as compared to the yedoma OM. The obtained findings are consistent with high bioavailability of OM in yedoma thaw waters (Drake et al., 2018; Vonk et al., 2013).

The specific features of compositional space inherent within the immobile alkali-extracted OM isolated from the yedoma and alas cores were revealed using FT-ICR MS analysis. It was shown (Figure 3) that all FA fractions were dominated by the oxidized species with O/C > 0.6, commonly referred to as hydrolyzable tannins (Perminova, 2019). The abundance of these constituents might be connected to intense oxidation of lignin, buried in the Siberian yedoma (Davydov et al., 2011), by active oxygen species. It has been reported that radical oxidation of lignins might lead to formation of partly reduced polyphenolic structures (Waggoner et al., 2017; Zherebker et al., 2015). In addition, the same high O/C values are characteristic to polycarboxylic aromatic acids (Zherebker et al., 2017). This indicates that during the onset of the thaw season (e.g., spring freshet), FA could be released into the environment and exported into the Kolyma River as a major terrestrial component of DOM. This is supported by the UV-visible absorbance and fluorescence measurements during the months dominated by surface soil and vegetation-derived OM inputs (Mann et al., 2012). On the contrary to FA, HA fractions from both cores were dominated by relatively reduced components, which might be attributed to lignins (H/C < 1.6), aliphatic species (H/C > 1.6), and low-oxidized aromatic compounds (H/C < 1). The aliphatic CHO species might be derived from the microbial degradation of plant terpenoids (Simpson et al., 2011). Oxidative cleavage of lignin could also contribute to formation of carboxyl-containing aliphatic molecular formula (DiDonato et al., 2016). The latter mechanism is also consistent with the lignin abundance in HA samples.

The quantitative comparison of the occupation density of the six chemical class-specific areas on the van Krevelen diagram (Figure 4) enabled us to reveal the origin-specific molecular features of the alkali-extracted OM from the yedoma core versus the alas one. For HA representing the most abundant fraction of this OM (Table 1), it was the presence of N-containing saturated compounds usually referred to as aliphatic amines, peptides, and amino sugars (Roth et al., 2015), whose content increased with depth in the yedoma core, being negligibly small in the alas core. In addition, the much higher content of saturated CHO species (aliphatics) was observed in the yedoma HA fractions as compared to the alas ones. Together with the highest C_{HA}/C_{FA} values determined for the deep alas samples under study, the above data on molecular composition are indicative of the more humified (aromatic and oxidized) character of immobile OM accumulated in the deep alas core as compared to the much more biolabile N-rich and saturated OM of the deep yedoma core. Such trends appear sensible given the genesis of alas OM formation under conditions of the thermokarst lake when the yedoma OM undergoes intense anaerobic and aerobic degradation (Webb et al., 2017). Such genesis should be reflected in the evolution of the compositional space of OM from the leading contribution of biolabile saturated compounds toward oxidized species. Of particular importance is that this evolutionary trend can be clearly seen in HA fractions, which are composed of the least transformed, structurally heterogeneous components of immobile OM, and it is becoming almost indiscernible in the most transformed, more homogeneous, and highly oxidized FA fractions of immobile OM.

4.2. Statistical Assessment of the Data on Molecular Composition of the HA and FA Fractions

The statistical assessment of the trends described above in the molecular compositions of HA versus FA fractions from the yedoma and alas cores shows that within each HCA cluster (Figure 5b), we observed the highest similarity within the permafrost type: alas or yedoma. The only exception was the grouping of the yedoma FA2 fraction from 6-m depth (FA-Y-6.2) with the alas FA2 fractions from 13 and 15.5 m. This could be indicative of a higher similarity of the surface yedoma with the deep alas layer. Accordingly, the molecular heatmap (Figure 5a) revealed the higher similarity of alas fractions to each other and to the upper-layer of yedoma as compared to the deep yedoma, which is supportive of the HCA results. The PCA on Boolean fingerprints demonstrated the leading contribution of saturated low oxidized components into HA versus FA1 and FA2 fractions (Figure 6) for both types of deposits studied. Furthermore, the use of peak intensities

instead of the presence/absence fingerprints for the PCA matrices enabled us to distinguish between both FA2 and HA fractions isolated from the alas and yedoma cores (Figure 7). This was not possible to do for FA2 fractions by the simple comparison of population density of the compounds-specific areas of van Krevelen diagrams. Overall, the study results demonstrate a great promise of molecular exploration of alkali-extracted OM, traditionally referred to as HSs, and, in particular, of its HA fraction, for revealing evolutionary trends in the compositional space of the permafrost OM during the repeated warming and refreezing conditions characteristic for formation of the thermokarst lakes. These trends might have important implications for prediction of the fate of permafrost OM under the current scenario of climate change.

5. Conclusions

The presented study provides the first insights into the evolution of the compositional space of the alkali-extracted immobile OM stored within the diagenetically connected yedoma and alas deposits of the thermokarst lake (Shchuchye Lake near Chersky settlement, Yakutia, Russia). The clear loss of aliphatic CHO and N-containing molecular formulae from the molecular assemblage of yedoma OM was revealed during its transformation under conditions of the thermokarst lake genesis leading to formation of much more aromatic and oxidized OM in the alas deposits. The observed changes are consistent with intense microbial degradation of energy rich and biolabile components of the yedoma deposits and accumulation of plant-derived highly transformed OM in the alas deposits. The undertaken isolation of HA fractions, which represent the most abundant portions of the total OC stored in the both yedoma and alas cores used in this study (up to 50% of OC), enabled us to observe the best imprint of these evolutionary changes in compositional space of OM: They were hardly discernible upon analysis of the much more transformed and less abundant fractions of FAs. The obtained results enhance our knowledge on the molecular evolution of OM during past and future thaw events, which can contribute to improved both paleoreconstructions and better predictions of climate feedback to transformation of the released OM due to permafrost thaw.

Competing Financial Interest

The authors declare no competing financial interests.

Acknowledgments
This work was partially supported by the Russian Foundation for Basic Research in part of isolation and fractionation of organic matter into fulvic and humic fractions and data treatment (Grant 16-04-01753 and 18-29-25065, respectively). The high-resolution mass spectrometry study was funded by the Russian Science Foundation Grant 19-14-00306 and partially supported by NSF (DMR-1157490), the State of Florida, and the FSU Future Fuels Institute. The statistical treatment of the results was a part of the Russian Science Foundation project (16-14-00167). Data on molecular class distribution obtained by FT-ICR MS analysis for all samples are provided in the supporting information online.

References

Anthony, K. M. W., Zimov, S. A., Grosse, G., Jones, M. C., Anthony, P. M., Chapin, F. S. III, et al. (2014). A shift of thermokarst lakes from carbon sources to sinks during the Holocene epoch. *Nature*, *511*(7510), 452–456. https://doi.org/10.1038/nature13560

Choi, J. H., Kim, Y.-G., Lee, Y. K., Pack, S. P., Jung, J. Y., & Jang, K.-S. (2017). Chemical characterization of dissolved organic matter in moist acidic tussock tundra soil using ultra-high resolution 15T FT-ICR mass spectrometry. *Biotechnology and Bioprocess Engineering*, *22*(5), 637–646. https://doi.org/10.1007/s12257-017-0121-4

D'Andrilli, J., Foreman, C. M., Marshall, A. G., & McKnight, D. M. (2013). Characterization of IHSS Pony Lake fulvic acid dissolved organic matter by electrospray ionization Fourier transform ion cyclotron resonance mass spectrometry and fluorescence spectroscopy. *Organic Geochemistry*, *65*, 19–28. https://doi.org/10.1016/j.orggeochem.2013.09.013

Davydov, S., Vonk, J. E., Mann, P. J., Davydova, A., Sobczak, W. V, Schade, J. D., et al. (2011). Reactivity of Pleistocene aged organic matter in the Siberian Arctic. In AGU Fall Meeting Abstracts.

DiDonato, N., Chen, H., Waggoner, D., & Hatcher, P. G. (2016). Potential origin and formation for molecular components of humic acids in soils. *Geochimica et Cosmochimica Acta*, *178*, 210–222. https://doi.org/10.1016/j.gca.2016.01.013

Dittmar, T., Koch, B., Hertkorn, N., & Kattner, G. (2008). A simple and efficient method for the solid-phase extraction of dissolved organic matter (SPE-DOM) from seawater. *Limnology and Oceanography: Methods*, *6*(6), 230–235. https://doi.org/10.4319/lom.2008.6.230

Drake, T. W., Guillemette, F., Hemingway, J. D., Chanton, J. P., Podgorski, D. C., Zimov, N. S., & Spencer, R. G. M. (2018). The ephemeral signature of permafrost carbon in an Arctic fluvial network. *Journal of Geophysical Research: Biogeosciences*, *123*, 1475–1485. https://doi.org/10.1029/2017JG004311

Hertkorn, N., Ruecker, C., Meringer, M., Gugisch, R., Frommberger, M., Perdue, E. M., et al. (2007). High-precision frequency measurements: Indispensable tools at the core of the molecular-level analysis of complex systems. *Analytical and Bioanalytical Chemistry*, *389*(5), 1311–1327. https://doi.org/10.1007/s00216-007-1577-4

Hockaday, W. C., Purcell, J. M., Marshall, A. G., Baldock, J. A., & Hatcher, P. G. (2009). Electrospray and photoionization mass spectrometry for the characterization of organic matter in natural waters: a qualitative assessment. *Limnology and Oceanography*, *7*, 81–95.

Kaiser, N. K., Quinn, J. P., Blakney, G. T., Hendrickson, C. L., & Marshall, A. G. (2011). A novel 9.4 tesla FTICR mass spectrometer with improved sensitivity, mass resolution, and mass range. *Journal of the American Society for Mass Spectrometry*, *22*(8), 1343–1351. https://doi.org/10.1007/s13361-011-0141-9

Koch, B. P., Witt, M., Engbrodt, R., Dittmar, T., & Kattner, G. (2005). Molecular formulae of marine and terrigenous dissolved organic matter detected by electrospray ionization Fourier transform ion cyclotron resonance mass spectrometry. *Geochimica et Cosmochimica Acta*, *69*(13), 3299–3308. https://doi.org/10.1016/j.gca.2005.02.027

Kunenkov, E. V., Kononikhin, A. S., Perminova, I. V., Hertkorn, N., Gaspar, A., Schmitt-Kopplin, P., et al. (2009). Total mass difference statistics algorithm: A new approach to identification of high-mass building blocks in electrospray ionization fourier transform ion

cyclotron mass spectrometry data of natural organic matter. *Analytical Chemistry*, *81*(24), 10,106–10,115. https://doi.org/10.1021/ac901476u

Lam, B., Baer, A., Alaee, M., Lefebvre, B., Moser, A., Williams, A., & Simpson, A. J. (2007). Major structural components in freshwater dissolved organic matter. *Environmental Science & Technology*, *41*(24), 8240–8247. https://doi.org/10.1021/es0713072

Mann, P. J., Davydova, A., Zimov, N., Spencer, R. G. M., Davydov, S., Bulygina, E., et al. (2012). Controls on the composition and lability of dissolved organic matter in Siberia's Kolyma River basin. *Journal of Geophysical Research*, *117*, G01028. https://doi.org/10.1029/2011JG001798

Mann, B. F., Chen, H., Herndon, E. M., Chu, R. K., Tolic, N., Portier, E. F., et al. (2015). Indexing permafrost soil organic matter degradation using high-resolution mass spectrometry. *PLoS One*, *10*(6), e0130557. https://doi.org/10.1371/journal.pone.0130557

Marshall, A. G., Hendrickson, C. L., & Jackson, G. S. (1998). Fourier transform ion cyclotron resonance mass spectrometry: A primer. *Mass Spectrometry Reviews*, *17*(1), 1–35. https://doi.org/10.1002/(SICI)1098-2787(1998)17:1<1::AID-MAS1>3.0.CO;2-K

Nikolaev, E. N., Boldin, I. A., Jertz, R., & Baykut, G. (2011). Initial experimental characterization of a new ultra-high resolution FTICR cell with dynamic harmonization. *Journal of The American Society for Mass Spectrometry*, *22*(7), 1125–1133. https://doi.org/10.1007/s13361-011-0125-9

O'Donnell, J. A., Aiken, G. R., Butler, K. D., Guillemette, F., Podgorski, D. C., & Spencer, R. G. M. (2016). DOM composition and transformation in boreal forest soils: The effects of temperature and organic-horizon decomposition state. *Journal of Geophysical Research: Biogeosciences*, *121*, 2727–2744. https://doi.org/10.1002/2016JG003431

Perminova, I. V. (2019). From green chemistry and nature-like technologies towards ecoadaptive chemistry and technology. *Pure and Applied Chemistry*, *91*(5), 851–864. https://doi.org/10.1515/pac-2018-1110

Perminova, I. V., Dubinenkov, I. V., Kononikhin, A. S., Konstantinov, A. I., Zherebker, A. Y., Andzhushev, M. A., et al. (2014). Molecular mapping of sorbent selectivities with respect to isolation of arctic dissolved organic matter as measured by fourier transform mass spectrometry. *Environmental Science and Technology*, *48*(13), 7461–7468. https://doi.org/10.1021/es5015423

Qualls, R. G., & Haines, B. L. (1992). Biodegradability of dissolved organic matter in forest throughfall, soil solution, and stream water. *Soil Science Society of America Journal*, *56*(2), 578–586. https://doi.org/10.2136/sssaj1992.03615995005600020038x

Rossel, P. E., Vähätalo, A. V., Witt, M., & Dittmar, T. (2013). Molecular composition of dissolved organic matter from a wetland plant (Juncus effusus) after photochemical and microbial decomposition (1.25 yr): Common features with deep sea dissolved organic matter. *Organic Geochemistry*, *60*, 62–71. https://doi.org/10.1016/j.orggeochem.2013.04.013

Roth, V. N., Dittmar, T., Gaupp, R., & Gleixner, G. (2015). The molecular composition of dissolved organic matter in forest soils as a function of pH and temperature. *PLoS ONE*, *10*(3), e0119188. https://doi.org/10.1371/journal.pone.0119188

Schirrmeister, L., Grosse, G., Wetterich, S., Overduin, P. P., Strauss, J., Schuur, E. A. G., & Hubberten, H. W. (2011). Fossil organic matter characteristics in permafrost deposits of the northeast Siberian Arctic. *Journal of Geophysical Research*, *116*, G00M02. https://doi.org/10.1029/2011JG001647

Shirshova, L. T., Kholodov, A. L., Zolotareva, B. N., Fominykh, L. A., & Yermolayev, A. M. (2009). Fluorescence spectroscopy studies of humic substance fractions isolated from permanently frozen sediments of Yakutian coastal lowlands. *Geoderma*, *149*(1–2), 116–123. https://doi.org/10.1016/j.geoderma.2008.11.026

Shmelev, D., Veremeeva, A., Kraev, G., Kholodov, A., Spencer, R. G. M., Walker, W. S., & Rivkina, E. (2017). Estimation and sensitivity of carbon storage in permafrost of north-eastern Yakutia. *Permafrost and Periglacial Processes*, *28*(2), 379–390. https://doi.org/10.1002/ppp.1933

Siewert, M. B., Hanisch, J., Weiss, N., Kuhry, P., Maximov, T. C., & Hugelius, G. (2015). Comparing carbon storage of Siberian tundra and taiga permafrost ecosystems at very high spatial resolution. *Journal of Geophysical Research: Biogeosciences*, *120*, 1973–1994. https://doi.org/10.1002/2015JG002999

Simpson, A. J., McNally, D. J., & Simpson, M. J. (2011). NMR spectroscopy in environmental research: From molecular interactions to global processes. *Progress in Nuclear Magnetic Resonance Spectroscopy*, *58*(3-4), 97–175. https://doi.org/10.1016/j.pnmrs.2010.09.001

Sleighter, R. L., Liu, Z., Xue, J., & Hatcher, P. G. (2010). Multivariate statistical approaches for the characterization of dissolved organic matter analyzed by ultrahigh resolution mass spectrometry. *Environmental Science and Technology*, *44*(19), 7576–7582. https://doi.org/10.1021/es1002204

Spencer, R. G. M., Mann, P. J., Dittmar, T., Eglinton, T. I., McIntyre, C., Holmes, R. M., et al. (2015). Detecting the signature of permafrost thaw in Arctic rivers. *Geophysical Research Letters*, *42*, 2830–2835. https://doi.org/10.1002/2015GL063498

Stevenson, F. J. (1995). Humus chemistry: Genesis, composition, reactions, second edition (Stevenson, F. J.). *Journal of Chemical Education*, *72*(4), A93. https://doi.org/10.1021/ed072pA93.6

Strauss, J., Schirrmeister, L., Grosse, G., Fortier, D., Hugelius, G., Knoblauch, C., et al. (2017). Deep Yedoma permafrost: A synthesis of depositional characteristics and carbon vulnerability. *Earth-Science Reviews*, *172*, 75–86. https://doi.org/10.1016/j.earscirev.2017.07.007

Strauss, J., Schirrmeister, L., Grosse, G., Wetterich, S., Ulrich, M., Herzschuh, U., & Hubberten, H. W. (2013). The deep permafrost carbon pool of the Yedoma region in Siberia and Alaska. *Geophysical Research Letters*, *40*, 6165–6170. https://doi.org/10.1002/2013GL058088

Stubbins, A., Mann, P. J., Powers, L., Bittar, T. B., Dittmar, T., McIntyre, C. P., et al. (2017). Low photolability of yedoma permafrost dissolved organic carbon. *Journal of Geophysical Research: Biogeosciences*, *122*, 200–211. https://doi.org/10.1002/2016JG003688

Swift, R. S. (1996). Organic matter characterization. In D. L. Sparks, A. L. Page, P. A. Helmke, R. H. Loeppert, P. N. Soltanpour, M. A. Tabatabai, & C. T. Johnson (Eds.), *Methods of soil analysis. Part 3. Chemical methods* (pp. 1011–1069). Madison, WI: SSSA Book Series no. 5.

Tamocai, C., Canadell, J. G., Schuur, E. A. G., Kuhry, P., Mazhitova, G., & Zimov, S. (2009). Soil organic carbon pools in the northern circumpolar permafrost region. *Global Biogeochemical Cycles*, *23*, GB2023. https://doi.org/10.1029/2008GB003327

Tesi, T., Muschitiello, F., Smittenberg, R. H., Jakobsson, M., Vonk, J. E., Hill, P., et al. (2016). Massive remobilization of permafrost carbon during post-glacial warming. *Nature Communications*, *7*, 13653. https://doi.org/10.1038/ncomms13653

Vasilevich, R., Lodygin, E., Beznosikov, V., & Abakumov, E. (2018). Molecular composition of raw peat and humic substances from permafrost peat soils of European Northeast Russia as climate change markers. *Science of the Total Environment*, *615*, 1229–1238. https://doi.org/10.1016/j.scitotenv.2017.10.053

Vonk, J. E., Mann, P. J., Dowdy, K. L., Davydova, A., Davydov, S. P., Zimov, N., et al. (2013). Dissolved organic carbon loss from Yedoma permafrost amplified by ice wedge thaw. *Environmental Research Letters*, *8*(3), 035023. https://doi.org/10.1088/1748-9326/8/3/035023

Vonk, J., Tank, S., Mann, P., Spencer, R., Treat, C., Striegl, R., et al. (2015). Biodegradability of dissolved organic carbon in permafrost soils and aquatic systems: a meta-analysis. *Biogeosciences*, *12*(23), 6915–6930. http://doi.org/10.5194/bg-12-6915-2015

Waggoner, D. C., Wozniak, A. S., Cory, R. M., & Hatcher, P. G. (2017). The role of reactive oxygen species in the degradation of lignin derived dissolved organic matter. *Geochimica et Cosmochimica Acta*, *208*, 171–184. https://doi.org/10.1016/j.gca.2017.03.036

Webb, E. E., Heard, K., Natali, S. M., Bunn, A. G., Alexander, H. D., Berner, L. T., et al. (2017). Variability in above- and belowground carbon stocks in a Siberian larch watershed. *Biogeosciences*, *14*(18), 4279–4294. https://doi.org/10.5194/bg-14-4279-2017

Zherebker, A., Kostyukevich, Y., Kononikhin, A., Kharybin, O., Konstantinov, A. I., Zaitsev, K. V., et al. (2017). Enumeration of carboxyl groups carried on individual components of humic systems using deuteromethylation and Fourier transform mass spectrometry. *Analytical and Bioanalytical Chemistry*, *409*(9), 2477–2488. https://doi.org/10.1007/s00216-017-0197-x

Zherebker, A. Y., Airapetyan, D., Konstantinov, A. I., Kostyukevich, Y. I., Kononikhin, A. S., Popov, I. A., et al. (2015). Synthesis of model humic substances: A mechanistic study using controllable H/D exchange and Fourier transform ion cyclotron resonance mass spectrometry. *Analyst*, *140*(13), 4708–4719. https://doi.org/10.1039/c5an00602c

Zherebker, A. Y., Perminova, I. V., Konstantinov, A. I., Volikov, A. B., Kostyukevich, Y. I., Kononikhin, A. S., & Nikolaev, E. N. (2016). Extraction of humic substances from fresh waters on solid-phase cartridges and their study by Fourier transform ion cyclotron resonance mass spectrometry. *Journal of Analytical Chemistry*, *71*(4), 372–378. https://doi.org/10.1134/S1061934816040109

Zhu, D., Peng, S., Ciais, P., Zech, R., Krinner, G., Zimov, S., & Grosse, G. (2016). Simulating soil organic carbon in yedoma deposits during the Last Glacial Maximum in a land surface model. *Geophysical Research Letters*, *43*, 5133–5142. https://doi.org/10.1002/2016GL068874

Zimov, S. A., Davydov, S. P., Zimova, G. M., Davydova, A. I., Schuur, E. A. G., Dutta, K., & Chapin, I. S. (2006). Permafrost carbon: Stock and decomposability of a globally significant carbon pool. *Geophysical Research Letters*, *33*, L20502. https://doi.org/10.1029/2006GL027484

Zimov, S. A., Schuur, E. A. G., & Chapin, F. S. (2006). Permafrost and the global carbon budget. *Science*, *312*(5780), 1612–1613. https://doi.org/10.1126/science.1128908